Direct Observation of the Superfluid Phase Transition in Ultracold Fermi Gases

Martin W. Zwierlein, Christian H. Schunck, André Schirotzek, and Wolfgang Ketterle

Supplementary Information

Supplementary Figures

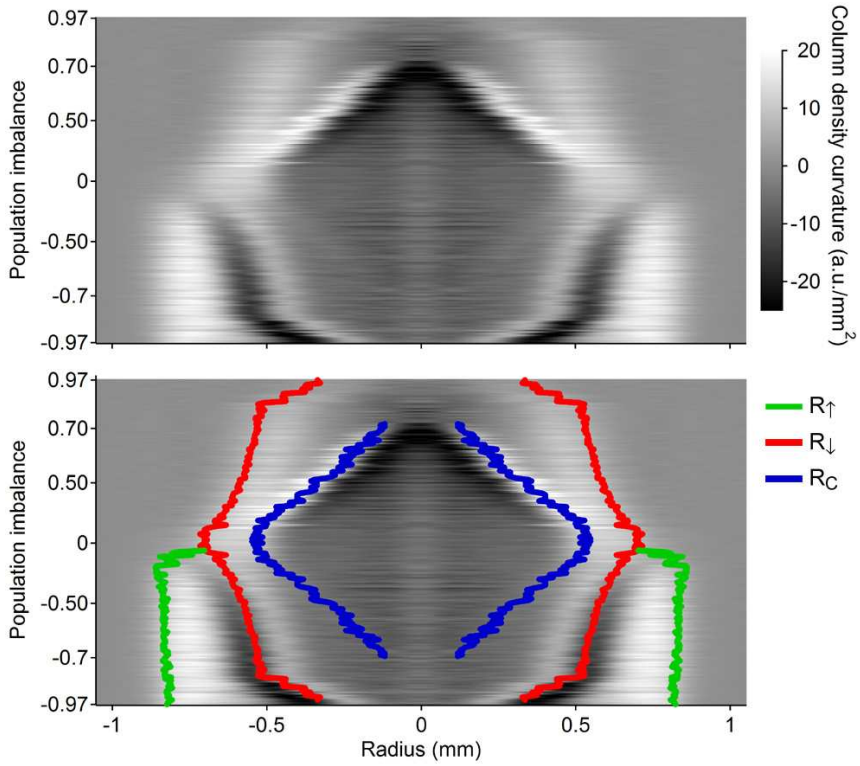

Supplementary Figure 1: (Color online) Signatures of the condensate on resonance in the spatial profiles. The curvature of the observed column density is encoded in shades of gray with white (black) corresponding to positive (negative) curvature. The outer radii of the two components and the condensate radius are shown as an overlay in the lower panel. As a direct consequence of strong interactions, the minority component causes a pronounced bulge in the majority density that is reflected in the rapid variation of the profile's curvature. The condensate is clearly visible in the minority component ($\delta > 0$), but also leaves a faint trace in the majority component ($\delta < 0$). The image was composed out of 216 individual azimuthally averaged column density profiles, smoothed to reduce technical noise. Data close to the cloud's center suffer from larger noise due to the lower number of averaged points. The central feature of about 50μm width is an artefact of smoothing in this region of increased noise.

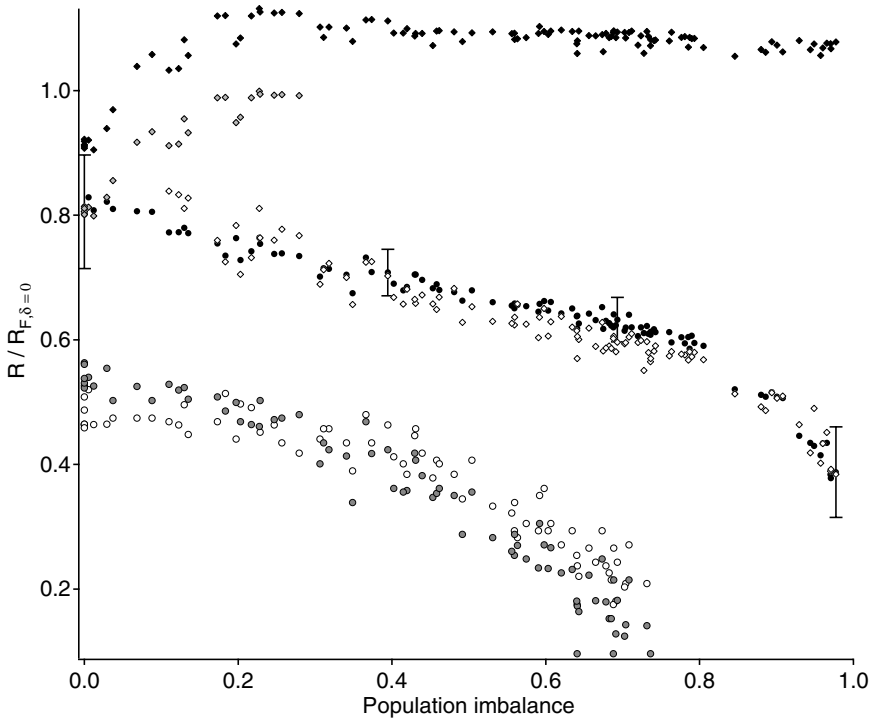

Supplementary Figure 2: Outer radii of the two cloud profiles and condensate radius versus population imbalance. Data obtained from the majority (minority) cloud are shown as diamonds (circles). The outer radii of the clouds (black) are determined from Thomas-Fermi fits to the profiles' wings, where the results of a zero-temperature and a finite temperature fit were averaged. For the minority cloud, the representative error bars indicate the difference between these two results. The position of the "bulge" in the majority profile (white diamonds) naturally follows the outer minority radius. The condensate radius is defined as the position of the "kink" in the minority profiles. It was obtained by a) fitting an increasing portion of the minority wings until a significant increase in χ^2 was observed (grey circles), and b) the position of the minimum in the profile's derivative (white circles). All sizes are scaled by the Fermi-radius of a non-interacting equal mixture. The minority radii were adjusted for the observed hydrodynamic expansion (expansion factor 11.0). The non-interacting wings of the majority cloud expand ballistically (expansion factor 9.7), as long as they are found a factor $11/9.7 = 1.13$ further out than the minority radius. For small imbalances ($\delta < 20\%$), also the majority wing's expansion will be affected by collisions. The grey diamonds give the majority cloud's outer radius if hydrodynamic expansion is assumed.

Supplementary Methods

Hydrodynamic vs. ballistic expansion

A non-interacting cloud of atoms simply expands ballistically from a trap. However, strongly interacting equal Fermi mixtures, above and below the phase transition, are collisionally dense and therefore expand according to hydrodynamic scaling laws [1–3]. These scaling laws only depend on the equation of state of the gas, $\epsilon \propto n^\gamma$, with $\gamma = 1$ for the BEC-side, $\gamma = 2/3$ for resonance (a direct consequence of unitarity) and $\gamma = 2/3$ for the BCS-side, away from resonance. In an unequal spin mixture of fermions, the expansion does not follow a simple scaling law. The minority cloud is always in contact with majority atoms and thus strongly interacting throughout the expansion, which is therefore hydrodynamic. The excess atoms in the wings of the larger cloud are non-interacting and will expand ballistically, as we have checked experimentally. The absorption images after expansion are taken along the axial direction of the trap (the direction of the optical trapping beam). In order to compare the expanded cloud sizes to the in-trap Fermi radii of non-interacting clouds (see Fig. 2 and Fig. S2 below) we scale the majority cloud with the ballistic factor for the radial direction

$$\sqrt{\cosh^2\left(2\pi\nu_z t/\sqrt{2}\right) + (\sqrt{2}\nu_r/\nu_z)^2 \sinh^2\left(2\pi\nu_z t/\sqrt{2}\right)},$$

where t is the expansion time and $\nu_z/\sqrt{2}$ gives the radial anti-trapping curvature of the magnetic saddle-point potential. The scaling factor for the hydrodynamic expansion of an equal mixture is given by the solution to a differential equation [2,3]. A priori, the minority cloud in unequal mixtures could expand with a different scaling, since the equation of state now depends on *two* densities. However, by imaging the cloud in trap and at different times during expansion, we found that the minority cloud's expansion is very well described by the scaling law for an equal mixture. In particular, the aspect ratio of the minority cloud did not change as a function of population imbalance (within our experimental error of 5%), and was equal to that of a balanced mixture.

For the data on resonance in Figs. 3, S1 and S2, which were obtained after 11 ms expansion out of a trap with radial (axial) frequency of $\nu_r = 113(10)\,\mathrm{Hz}$ ($\nu_z = 22.8(0.2)\,\mathrm{Hz}$), the ballistic (hydrodynamic) expansion factor for the radial direction is 9.7 (11.0).

Supplementary Discussion

Signature of the condensate

Fig. S1 demonstrates that on resonance, the condensate is visible not only in the minority component, but also in the larger cloud as a small change in the profile's curvature. In the condensate region, the majority profile is slightly depleted when compared to the shape of a normal Fermi cloud. This effect is still significant on the BCS-side (see Fig. 1): Although here, the condensate is less visible in the smaller component than on resonance, the larger cloud's central depletion still produces a clear dip in the difference profile.

Radii in the unequal Fermi mixture

Fig. S2 shows the outer radii of the majority and minority cloud, together with the condensate radius (on resonance, for the deepest evaporation compatible with constant total atom number versus imbalance). As was the case for the phase transition at finite temperature, the outer cloud sizes change smoothly with imbalance. No drastic change is seen at the critical population imbalance. The radii are obtained by fitting the profiles' wings to the Thomas-Fermi expression for the radial column density $n(r)$:

$$n(r) = n_0 \frac{\mathrm{Li}_2\left(-\lambda^{1-r^2/R^2}\right)}{\mathrm{Li}_2\left(-\lambda\right)},$$

with the central column density n_0, the fugacity λ and the Thomas-Fermi radius R as the free parameters. $\mathrm{Li}_2(x)$ is the Dilogarithm. The zero-temperature expression reduces to $n(r) = n_0(1 - r^2/R^2)^2$.

Lower and upper bounds for the critical chemical potential difference at δ_c

For the clouds at the critical imbalance δ_c, we now want to extract a lower and upper bound for the difference in chemical potentials $\delta\mu_c$ of the majority and minority component. This difference allows us to conclude that BCS-type superfluidity with imbalanced densities is not possible.

The chemical potential difference $\delta\mu \equiv 2h = (\mu_\uparrow - \mu_\downarrow)$ measures the energy cost, relative to $\mu = (\mu_\uparrow + \mu_\downarrow)/2$, to add a particle to the cloud of excess fermions. Δ, the pairing gap, is the energy cost for this additional majority particle to enter the superfluid. Both the critical temperature T_C and the critical chemical potential difference $\delta\mu_c$ provide a measure of the superfluid gap: The superfluid can be either destroyed by raising the temperature or by increasing the population imbalance. If $h_c \equiv \delta\mu_c/2 < \Delta$, excess atoms will always stay outside the superfluid, in the phase separated normal state. For $h_c > \Delta$, excess atoms can enter the superfluid for $h_c > h > \Delta$. Hence, superfluidity with unequal densities, if allowed via $h_c > \Delta$, would be favored at large population imbalance, contrary to the interpretation in [4], where such a state was proposed for small population imbalance. A recent Monte-Carlo calculation [5] for the Clogston limit on resonance gives $h_c = 1.00(5)\Delta = 0.50(5)E_F$ and can thus not decide on the question of superfluidity with imbalanced densities.

We can attempt to extract the chemical potential from the cloud sizes $R_{\uparrow,\downarrow}$ - taking into account hydrodynamic expansion for the minority cloud and ballistic expansion for the excess fermions. For the majority cloud, we find $\mu_{c,\uparrow} = 1/2\, m\omega_r^2 R_\uparrow^2 = 1.21(6)E_F$. For the minority cloud, we find $1/2\, m\omega_r^2 R_\downarrow^2 = 0.39(10)E_F$. Throughout the smaller cloud, minority atoms are always strongly attracted by majority atoms. This strong attractive interaction likely reduces their chemical potential from the above upper limit. The difference of the chemical potentials $\delta\mu_c \equiv 2h_c$ is thus given by $h_c = (\mu_{c,\uparrow} - \mu_{c,\downarrow})/2 \geq 0.41(6)E_F = 0.51\mu$, our lower bound. Another condition on h_c concerns whether the normal state can be mixed, $h_c < \mu$, (minority and majority atoms in the same spatial region) or whether the normal state is always completely polarized $h_c > \mu$. Our observation of the mixed region in Fig. 1 immediately results in $h_c < \mu$, the upper bound.

On resonance, $\Delta = 1.16\mu$ in BCS-theory, while a recent Monte-Carlo study [5] obtains $\Delta = 1.2\mu$. If $\Delta > \mu$ holds true, our finding of the upper bound on h_c would imply $h_c < \Delta$ and hence would exclude a superfluid with unequal spin densities (at least on the basis of BCS-theory, see [6] for a recent suggestion which goes beyond BCS).

Supplementary Notes

1. O'Hara, K. M., Hemmer, S. L., Gehm, M. E., Granade, S. R. & Thomas, J. E. Observation of a strongly interacting degenerate fermi gas of atoms. *Science* **298**, 2179 (2002).

2. Menotti, C., Pedri, P. & Stringari, S. Expansion of an Interacting Fermi gas. *Phys. Rev. Lett.* **89**, 250402 (2002).

3. Castin, Y. Exact scaling transform for a unitary quantum gas in a time dependent harmonic potential. *Comptes Rendus Physique* **5**, 407–410 (2004).

4. Partridge, G. B., Li, W., Kamar, R. I., a. Liao, Y. & Hulet, R. G. Pairing and Phase Separation in a Polarized Fermi Gas. *Science* **311**, 503 (2006). Published online 21 December 2005 (10.1126/science.1122876).

5. Carlson, J. & Reddy, S. Asymmetric Two-Component Fermion Systems in Strong Coupling. *Phys. Rev. Lett.* **95**, 060401 (2005).

6. Ho, T.-L. & Zhai, H. Homogeneous Fermion Superfluid with Unequal Spin Populations. Preprint at <http://arxiv.org/cond-mat/0602568> (2006).